Electrical detection of nuclear spin-echo signals in an electron spin injection system

Zhichao Lin, Mahmoud Rasly, and Tetsuya Uemura

Citation: Appl. Phys. Lett. **110**, 232404 (2017); doi: 10.1063/1.4985650
View online: http://dx.doi.org/10.1063/1.4985650
View Table of Contents: http://aip.scitation.org/toc/apl/110/23
Published by the American Institute of Physics

Electrical detection of nuclear spin-echo signals in an electron spin injection system

Zhichao Lin, Mahmoud Rasly, and Tetsuya Uemura[a)]
Division of Electronics for Informatics, Graduate School of Information Science and Technology, Hokkaido University, Sapporo 060-0814, Japan

(Received 21 March 2017; accepted 31 May 2017; published online 8 June 2017)

We demonstrated spin echoes of nuclear spins in a spin injection device with a highly polarized spin source by nuclear magnetic resonance (NMR). Efficient spin injection into GaAs from a half-metallic spin source of Co_2MnSi enabled efficient dynamic nuclear polarization (DNP) and sensitive detection of NMR signals even at a low magnetic field of ~0.1 T and a relatively high temperature of 4.2 K. The intrinsic coherence time T_2 of ^{69}Ga nuclear spins was evaluated from the spin-echo signals. The relation between T_2 and the decay time of the Rabi oscillation suggests that the inhomogeneous effects in our system are not obvious. This study provides an all-electrical NMR system for nuclear-spin-based qubits. *Published by AIP Publishing.* [http://dx.doi.org/10.1063/1.4985650]

Quantum computation has attracted much interest in its powerful computing capacity. In a quantum computation system, the basic unit is a quantum bit (qubit). Unlike a conventional bit, a qubit can be in both 0 and 1 states, which is called a superposition state. It is this property that gives a quantum computation system the powerful ability of parallel computing. Nuclear spins are promising implementations for qubits because they have extremely long coherence times. The nuclear magnetic resonance (NMR) technique enables the control and detection of nuclear-spin-based qubits. However, the sensitivity of the conventional NMR technique is limited by the low magnetic moments of the nuclear spins, which are three orders of magnitude smaller than those of the electron spins. Dynamic nuclear polarization (DNP), where nuclear spins are dynamically polarized through a hyperfine interaction between nuclear spins and electron spins, has attracted much interest, since it can dramatically increase the NMR signal. Several instances of DNP in semiconductors induced by optical means or electrical means have been reported.[1–16] Furthermore, coherent manipulation of nuclear spins in semiconductors by NMR has been demonstrated electrically in GaAs/AlGaAs quantum Hall systems by observing the Rabi oscillation[17–19] and optically in GaAs/AlGaAs quantum wells by observing the Rabi oscillation and spin-echo signals.[20] Although the optical method is suitable for clarifying the fundamental physics of nuclear spins, it is restricted in its scalability because the spatial resolution is limited by the optical wavelength. The quantum Hall systems require a strong magnetic field of several tesla and a low temperature below 1 K to create highly polarized electron spins for DNP.

Recently, we developed an NMR system that uses spin injection from a highly polarized spin source and detected the Rabi oscillation electrically with a static magnetic field of ~0.1 T at 4.2 K.[21] A Mn-rich Co_2MnSi was used as a spin source because we demonstrated high tunneling magnetoresistance (TMR) ratios of up to 1995% at 4.2 K and up to 354% at 290 K in magnetic tunnel junctions (MTJs) having Mn-rich Co_2MnSi electrodes.[22] The obtained high TMR ratios for MTJs with Mn-rich Co_2MnSi electrodes are attributed to suppressed Co_{Mn} antisites, which leads to enhanced half-metallicity through a reduction in the density of minority-spin in-gap states around the Fermi level.[22–27] The demonstration of high TMR ratios indicates a high spin polarization of Mn-rich Co_2MnSi. Thus, the Mn-rich Co-based Heusler alloys are promising spin source materials for highly efficient spin injection into semiconductors. Indeed, we have demonstrated high-efficiency spin injection from Co_2MnSi into GaAs via an ultrathin insertion layer of CoFe in a spin injection device, resulting in an electron spin polarization of up to 52% at 4.2 K.[28] This enabled efficient DNP and sensitive detection of the Rabi oscillation even at a low magnetic field and a relatively high temperature.[21] Moreover, we clarified the transient response of nuclear spins against the change in magnetic field experimentally[16] and theoretically,[29,30] although most of the studies on DNP that have used electrical spin injection have been limited to static investigations,[11–13,15] in which the magnetic field was swept slowly enough for nuclear spins to reach their equilibrium.

For achieving nuclear-spin-based qubits, it is important to clarify the nuclear-spin phase coherence time T_2, because the lifetime of a qubit is limited by T_2. In our previous work,[21] we estimated T_2^{Rabi}, i.e., the decay time of the Rabi oscillation, in a spin injection device. Ideally, the intrinsic coherence time T_2 can be estimated from T_2^{Rabi} as $T_2 = T_2^{Rabi}/2$ when $T_1 \gg T_2$, where T_1 is the spin-lattice relaxation time of nuclear spins.[31–34] However, inhomogeneities in the external fields may enhance the decay of the Rabi oscillation, resulting in a decrease in T_2^{Rabi}. To exclude the inhomogeneous effects and estimate the intrinsic T_2, a spin-echo measurement,[20,33] which refocuses nuclear-spin magnetization by using a specific pulse sequence, has to be made. The purpose of the present study is to clarify the phase coherence time T_2 of the nuclear spins in GaAs through an electrical spin-echo measurement in a spin injection device. Since the durations of $\pi/2$ and π pulses should be determined when performing a spin-echo measurement, the Rabi oscillation was also measured, as was done in our previous work.[21]

a)E-mail: uemura@ist.hokudai.ac.jp

A lateral spin transport device having Co_2MnSi/CoFe/GaAs heterojunctions was fabricated (Fig. 1). The layer structure and device geometry are identical to the ones presented in Ref. 21. The device operation includes (1) Generation of spin-polarized electrons in GaAs by spin injection; (2) Initialization of nuclear spins by DNP; (3) Quantum manipulation of nuclear spins through the NMR effect; (4) Readout of nuclear spin states through the detection of the nonlocal voltage (V_{NL}) between electrode-3 and electrode-4. The nonlocal voltage is a measure of the response of the electron spins to the total magnetic field of both the nuclear field and external magnetic field. Through the NMR effect, the nuclear spins, or the nuclear field, are manipulated, resulting in the changes in the nonlocal voltage. Thus, the nuclear spin states can be read out from the changes of the nonlocal voltage (ΔV_{NL}). The creation, control, and detection of the nuclear spins in GaAs were evaluated in a four-terminal nonlocal geometry when V_{NL} between electrode-3 and electrode-4 was measured under a constant current I supplied between electrode-2 and electrode-1 under a static magnetic field $\mathbf{B}_0$ and an RF magnetic field $\mathbf{B}_{rf}$. The $\mathbf{B}_{rf}$ was generated by an 11-turn coil with a diameter of 1.0 cm for the NMR experiment. All the measurements were done at 4.2 K.

We observed clear spin-valve signals [Fig. 2(a)] and Hanle signals [Fig. 2(b)], which are direct evidence of spin injection from this device. The Hanle curves can be expressed as[35]

$$V_{NL} = \pm\frac{P_{inj}P_{det}}{2}\left(\rho\frac{l_{sf}}{S}\right)\left(\frac{2l_{sf}}{\tau_s}\right)I\int_0^\infty \frac{1}{\sqrt{4\pi Dt}} \times \exp\left(-\frac{d^2}{4Dt}\right)\cos\omega_L t\exp\left(-\frac{t}{\tau_S}\right)dt, \quad (1)$$

where $P_{inj(det)}$ is the spin polarization underneath the injector (detector) contact, ρ is the resistivity of the GaAs channel, S is the area of the channel cross-section, l_{sf} is the spin-diffusion length, d is the distance between contact-2 and contact-3, τ_S is the spin lifetime, $D = l_{sf}^2/\tau_S$ is the diffusion constant, and $\omega_L = g\mu_B B_z/\hbar$ is the Larmor frequency, where B_z is the z component of $\mathbf{B}_0$, g is an electron g-factor ($g = -0.44$ for GaAs), μ_B is the Bohr magneton, and $\hbar$ is the reduced Planck's constant. The sign of $+(-)$ on the right-hand side of Eq. (1) corresponds to the P (AP) configuration. The estimated values of τ_s, l_{sf}, and the effective spin polarization defined by

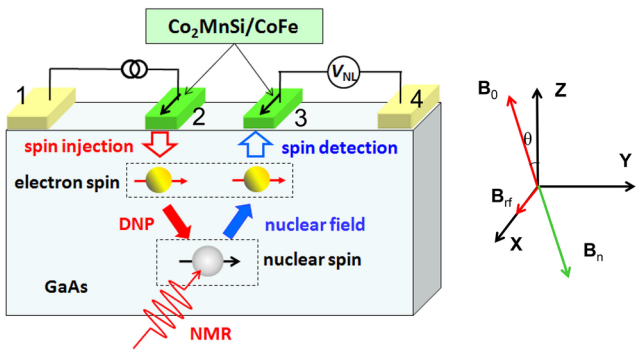

FIG. 1. Experimental setup of NMR for a lateral spin transport device. The injected electron spins are along the x-axis. Taking $\mathbf{B}_0\cdot\mathbf{S} > 0$ and $b_n < 0$ in Eq. (2) into consideration, $\mathbf{B}_n$ is anti-parallel to $\mathbf{B}_0$.

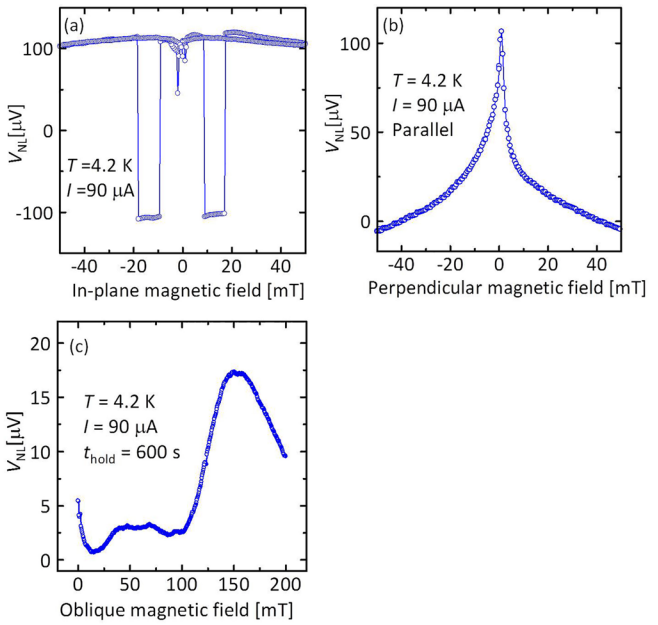

FIG. 2. (a) Spin-valve signals, (b) Hanle signals, and (c) Oblique Hanle signals measured at 4.2 K with a constant current $I = 90$ μA.

$|P_{inj}P_{det}|^{1/2}$ were $\tau_s = 20$ ns, $l_{sf} = 3$ μm, and $|P_{inj}P_{det}|^{1/2} = \sim 30\%$, respectively.

This high spin polarization in GaAs due to the spin injection from a highly polarized spin source of Co_2MnSi is promising for DNP. In order to check whether the DNP occurs in our device, the oblique Hanle signal [Fig. 2(c)] was measured. The magnetic field $\mathbf{B}_0$ ($|\mathbf{B}_0| = 200$ mT) was applied to the device along a direction tilted by a small angle $\theta \approx 8^\circ$ from the z-axis in the x–z plane for a holding time $t_{hold} = 600$ s, and then it was swept from 200 mT to 0 with a sweep rate of 0.4 mT/s. The generated nuclear field $\mathbf{B}_n$ is given by[36]

$$\mathbf{B}_n = f_l b_n \frac{\mathbf{B}_0\cdot\mathbf{S}}{\mathbf{B}_0^2 + \xi B_l^2}\mathbf{B}_0, \quad (2)$$

where f_l (≤ 1) is the leakage factor, b_n is the effective field due to the polarization of nuclear spins, which theoretically takes a negative value of -17 T in GaAs, $\mathbf{S}$ is the average electron spin ($|\mathbf{S}| = \frac{1}{2}$, corresponding to 100% polarization) under the detector contact, B_l is the local dipolar field experienced by the nuclei, and ξ is a numerical coefficient defined by the ratio of the nuclear spin polarization rate to the depolarization rate.[11] From Eq. (2), $\mathbf{B_n}$ and $\mathbf{B_0}$ are parallel or anti-parallel, depending on the sign of $b_n\mathbf{B}_0\cdot\mathbf{S}$. When $\mathbf{B_0} = \mathbf{0}$, $\mathbf{S}$ points along the x-axis, whereas when $\mathbf{B_0} \neq \mathbf{0}$, $\mathbf{S}$ precesses along $\mathbf{B}_0 + \mathbf{B}_n$. This precession changes only the component of $\mathbf{S}$ perpendicular to $\mathbf{B_0}$, and conserves the component of $\mathbf{S}$ parallel to $\mathbf{B_0}$, resulting in $\mathbf{B}_0\cdot\mathbf{S} > 0$ in this magnetic field configuration. Taking $b_n < 0$ in Eq. (2) into consideration, $\mathbf{B_n}$ is generated along the direction antiparallel to $\mathbf{B_0}$. The V_{NL} plotted in Fig. 2(c) can be described by Eq. (1) by replacing $\mathbf{B_0}$ with $\mathbf{B_0} + \mathbf{B_n}$. When $|\mathbf{B_0}|$ is swept from $+200$ mT to 0, $|\mathbf{B_0} + \mathbf{B_n}|$ reached a local minimum at $|\mathbf{B_0}| = 150$ mT, resulting in V_{NL} having a side peak at $|\mathbf{B_0}| = 150$ mT. In other words, the observation of the side peak is clear indication of DNP.

In the following, we describe the experimental results of the spin-echo measurement. First, we describe the initialization of the nuclear spins by DNP (Fig. 1). A static magnetic field $\mathbf{B}_0$ with a strength of $|\mathbf{B}_0| = 114$ mT was applied to the device along the direction tilted by a small angle $\theta \approx 8°$ from the z-axis in the x–z plane. Similar to the oblique Hanle signal measurement shown in Fig. 2(c), the electron spins injected from the Co_2MnSi spin source should polarize the nuclear spins through the DNP process, resulting in a nuclear field $\mathbf{B}_n$ being anti-parallel to $\mathbf{B}_0$.

Second, we describe the Rabi oscillation of ^{69}Ga nuclear spins by using a pulsed NMR to determine T_2^{Rabi} and durations for $\pi/2$ and π pulses. After the initialization of the nuclear spins, an RF magnetic field $\mathbf{B}_{\mathrm{rf}}$ was applied along the x-axis with a certain pulse duration τ_p and a frequency of 1118 kHz, corresponding to the resonance frequency of ^{69}Ga in a static magnetic field $|\mathbf{B}_0| = 114$ mT. Then, the nuclear spins of ^{69}Ga were rotated by an angle of $\gamma(^{69}\mathrm{Ga})|\mathbf{B}_{\mathrm{rf}}|\tau_p/2$ in the rotating frame which rotates along the z-axis with a rotating frequency synchronized to the resonance frequency of ^{69}Ga, where $\gamma(^{69}\mathrm{Ga})$ is the gyromagnetic ratio of ^{69}Ga. Consequently, the ^{69}Ga component of $\mathbf{B}_n$ was rotated, and the total magnetic field was changed, resulting in a change in V_{NL} according to Eq. (1). Figure 3(a) shows the time evolution of V_{NL} when $\mathbf{B}_{\mathrm{rf}}$ pulses with $\tau_p = 30$, 50, and 70 μs were applied at $t = 0$. V_{NL} increased rapidly by $\Delta V_{\mathrm{NL}} = 7$, 13, and 16 μV, respectively, and then it gradually recovered to its initial state on a time scale of several hundreds of seconds. The increase in V_{NL} due to the irradiation of the RF pulse indicates that the Hanle precession became weaker as a result of the decrease in the z component of the effective magnetic field, B_z. The value of B_z after the irradiation of a pulse with a duration of τ_p is given by

$$B_z(\tau_p) = A_1 \cos(2\pi f_{Rabi}\tau_p) \exp(-\tau_p/T_2^{Rabi}) - A_2, \qquad (3)$$

where A_1 and A_2 are constants, f_{Rabi} $(=\gamma(^{69}\mathrm{Ga})|\mathbf{B}_{\mathrm{rf}}|/4\pi)$ is the frequency for the oscillation of B_z, and T_2^{Rabi} is the effective dephasing time. We define ΔV_{NL} as the change in V_{NL} just after the $\mathbf{B}_{\mathrm{rf}}$ pulse. The oscillatory behavior of B_z induces an oscillation in ΔV_{NL} as a function of τ_p. Figure 3(b) shows the τ_p dependence of ΔV_N, along with a fitting curve calculated by substituting Eq. (3) into Eq. (1). We observed clear oscillations in ΔV_{NL} as a function of τ_p. From the fitting, $T_2^{\mathrm{Rabi}} = 320$ μs and $f_{\mathrm{Rabi}} = 5.4$ kHz were obtained, from which the amplitude of $\mathbf{B}_{\mathrm{rf}}$ was estimated to be $\sim$1 mT. The value of $T_2^{\mathrm{Rabi}} = 320$ μs was smaller than that of 400 μs previously reported in Ref. 21. This difference mainly owes to the enhancement of the dipole-dipole interactions accompanying a slight increase in θ from 5° to 8°, as was discussed in Ref. 20. From the period of the Rabi oscillation, the durations for $\pi/2$ and π pulses were determined to be 46 and 92 μs, respectively.

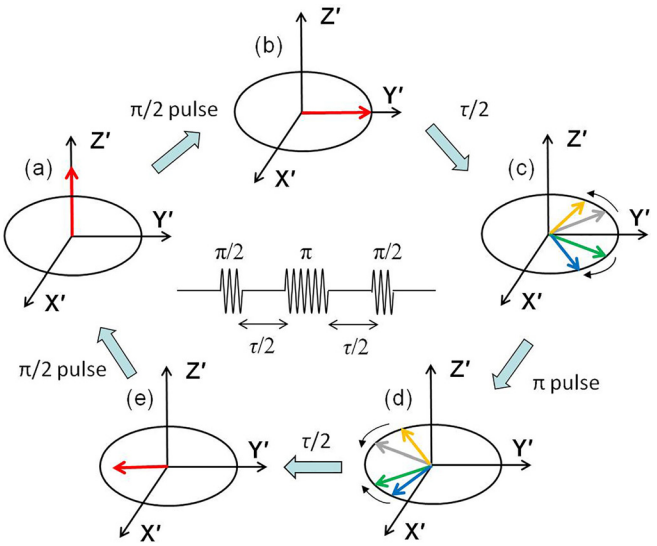

FIG. 4. Illustration of a spin-echo measurement in a rotating frame with a pulse sequence consisting of $\pi/2$, π, and $\pi/2$ pulses. The effective RF magnetic field is along the x'-axis.

Finally, we describe the spin-echo measurement. A series of pulses consisting of $\pi/2$, π, and $\pi/2$ pulses (Fig. 4) was applied to nuclear spins that were initialized to be along the z'-axis [Fig. 4(a)]. The first $\pi/2$ pulse rotates the nuclear spins by 90° to the y'-axis in the rotating frame [Fig. 4(b)], and the nuclear spins start to dephase because of both intrinsic interactions and inhomogeneities in the external fields. After a time of $\tau/2$ [Fig. 4(c)], the nuclear spins are flipped to the opposite side by application of a π pulse [Fig. 4(d)], and they start to refocus during the period of $\tau/2$. Then, a complete refocusing, or spin echo, occurs after $\tau/2$ [Fig. 4(e)]. The refocusing can occur because the dephasing due to the inhomogeneities in the external fields is reversible. Finally, the second $\pi/2$ pulse rotates the nuclear spins back to the z'-axis for readout [Fig. 4(a)]. Figure 5(a) shows the time evolution of V_{NL} when spin-echo pulse sequences with $\tau = 60$ and 200 μs were

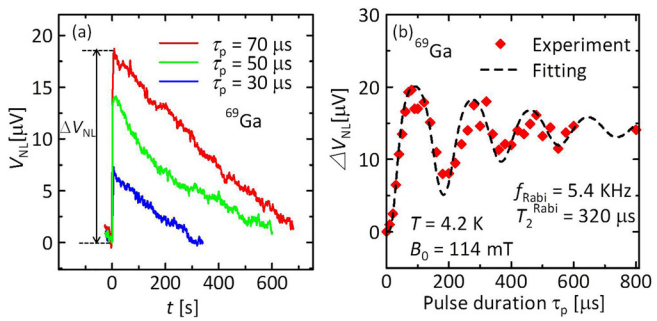

FIG. 3. (a) Time evolution of V_{NL} when $\mathbf{B}_{\mathrm{rf}}$ pulses with $\tau_p = 30$, 50, and 70 μs were applied at $t = 0$. V_{NL} was offset by 10.9 mV, so that $V_{\mathrm{NL}} = 0$ at $t = 0$. ΔV_{NL} is defined as the change in V_{NL} just after the $\mathbf{B}_{\mathrm{rf}}$ pulse. (b) τ_p dependence of ΔV_{NL} along with a fitting curve.

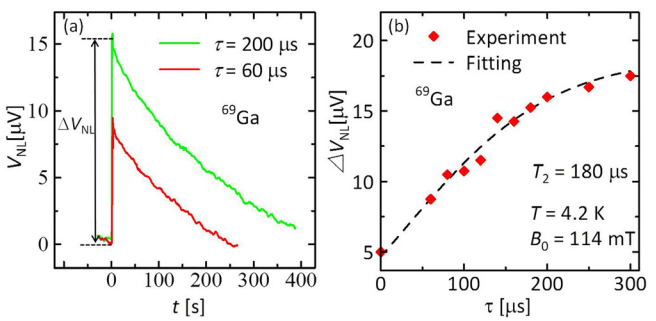

FIG. 5. (a) Time evolution of V_{NL} after applying spin-echo pulse sequence with $\tau = 60$ and 200 μs at $t = 0$. V_{NL} was offset by 10.9 mV, so that $V_{\mathrm{NL}} = 0$ at $t = 0$. (b) τ dependence of ΔV_{NL}. The offset of 5 μV at $\tau = 0$ results from the decay of the Rabi oscillation for one cycle.

applied at $t = 0$. V_{NL} changed rapidly by $\Delta V_{NL} = 8.5$ and $16\,\mu$V, respectively, after applying the pulse sequences; then it gradually recovered to its initial state. V_{NL} increased because the decay of ^{69}Ga nuclear spins resulted in a decrease in the z component of the effective magnetic field, which is given by

$$B_z(\tau) = A_3 \exp(-\tau/T_2) - A_4, \tag{4}$$

where A_3 and A_4 are constants. Figure 5(b) shows the τ dependence of ΔV_{NL}, along with a fitting curve calculated by substituting Eq. (4) into Eq. (1). An exponential-like behavior of ΔV_{NL}, corresponding to the intrinsic decoherence of ^{69}Ga nuclear spins, was observed. The intrinsic coherence time T_2 ($=180\,\mu$s) was obtained from the fitting results and is comparable with the values reported in Ref. 20.

Now, we will discuss the relation between the decay time of the Rabi oscillation T_2^{Rabi} and the intrinsic coherence time T_2. By solving the Bloch equations, one can get $T_2^{\text{Rabi}} = 2T_2$ when $T_1 \gg T_2$. This relation is valid only when the inhomogeneous effects are negligible. From the Rabi oscillation and spin-echo signals, $T_2^{\text{Rabi}} = 320\,\mu$s and $T_2 = 180\,\mu$s were obtained, and they satisfy the relation of $T_2^{\text{Rabi}} \sim 2T_2$. This suggests that the inhomogeneous effects in our measurement system are not obvious. This is reasonable because our device has nanoscale dimensions.

In conclusion, we demonstrated spin echoes of nuclear spins in a spin injection device with a highly polarized spin source. Efficient spin injection enabled efficient DNP and sensitive detection of spin-echo signals even at a low magnetic field of $\sim$0.1 T and a relatively high temperature of 4.2 K. This study is hence a big step towards achieving an all-electrical NMR system for nuclear-spin-based qubits.

The authors would like to thank Professors Masafumi Yamamoto and Kenji Kondo for their fruitful discussions. This work was partly supported by the Japan Society for the Promotion of Science (KAKENHI: Grant Nos. 25286039, 15K13960, 16K04872, and 17H03225).

[1]M. I. D'yakonov, V. I. Perel', V. L. Berkovits, and V. I. Safarov, Sov. Phys. - JETP **40**, 950 (1975).
[2]D. Paget, G. Lampel, B. Sapoval, and V. I. Safarov, Phys. Rev. B **15**, 5780 (1977).
[3]G. Lampel, Phys. Rev. Lett. **20**, 491 (1968).
[4]J. Strand, B. D. Schultz, A. F. Isakovic, C. J. Palmstrøm, and P. A. Crowell, Phys. Rev. Lett. **91**, 036602 (2003).
[5]D. Gammon, S. W. Brown, E. S. Snow, T. A. Kennedy, D. S. Katzer, and D. Park, Science **277**, 85 (1997).
[6]G. Salis, D. T. Fuchs, J. M. Kikkawa, and D. D. Awschalom, Phys. Rev. Lett. **86**, 2677 (2001).
[7]T. Machida, T. Yamazaki, and S. Komiyama, Appl. Phys. Lett. **80**, 4178 (2002).
[8]K. Hashimoto, K. Muraki, T. Saku, and Y. Hirayama, Phys. Rev. Lett. **88**, 176601 (2002).
[9]M. Poggio, G. M. Steeves, R. C. Myers, Y. Kato, A. C. Gossard, and D. D. Awschalom, Phys. Rev. Lett. **91**, 207602 (2003).
[10]K. Ono and S. Tarucha, Phys. Rev. Lett. **92**, 256803 (2004).
[11]J. Strand, X. Lou, C. Adelmann, B. D. Schultz, A. F. Isakovic, C. J. Palmstrøm, and P. A. Crowell, Phys. Rev. B **72**, 155308 (2005).
[12]P. Van Dorpe, W. Van Roy, J. De Boeck, and G. Borghs, Phys. Rev. B **72**, 035315 (2005).
[13]M. K. Chan, Q. O. Hu, J. Zhang, T. Kondo, C. J. Palmstrøm, and P. A. Crowell, Phys. Rev. B **80**, 161206(R) (2009).
[14]G. Salis, A. Fuhrer, and S. F. Alvarado, Phys. Rev. B **80**, 115332(R) (2009).
[15]J. Shiogai, M. Ciorga, M. Utz, D. Schuh, T. Arakawa, M. Kohda, K. Kobayashi, T. Ono, W. Wegscheider, D. Weiss, and J. Nitta, Appl. Phys. Lett. **101**, 212402 (2012).
[16]T. Akiho, J. Shan, H.-x. Liu, K.-i. Matsuda, M. Yamamoto, and T. Uemura, Phys. Rev. B **87**, 235205 (2013).
[17]T. Machida, T. Yamazaki, K. Ikushima, and S. Komiyama, Appl. Phys. Lett. **82**, 409 (2003).
[18]G. Yusa, K. Muraki, K. Takashina, K. Hashimoto, and Y. Hirayama, Nature **434**, 1001 (2005).
[19]H. Takahashi, M. Kawamura, S. Masubuchi, K. Hamaya, T. Machida, Y. Hashimoto, and S. Katsumoto, Appl. Phys. Lett. **91**, 092120 (2007).
[20]H. Sanada, Y. Kondo, S. Matsuzaka, K. Morita, C. Y. Hu, Y. Ohno, and H. Ohno, Phys. Rev. Lett. **96**, 067602 (2006).
[21]T. Uemura, T. Akiho, Y. Ebina, and M. Yamamoto, Phys. Rev. B **91**, 140410(R) (2015).
[22]H.-x. Liu, Y. Honda, T. Taira, K-i. Matsuda, M. Arita, T. Uemura, and M. Yamamoto, Appl. Phys. Lett. **101**, 132418 (2012).
[23]H.-x. Liu, T. Kawami, K. Moges, T. Uemura, M. Yamamoto, F. Shi, and P. M. Voyles, J. Phys. D: Appl. Phys. **48**, 164001 (2015).
[24]M. Yamamoto, T. Ishikawa, T. Taira, G.-f. Li, K.-i. Matsuda, and T. Uemura, J. Phys.: Condens. Matter **22**, 164212 (2010).
[25]G.-f. Li, Y. Honda, H.-x. Liu, K.-i. Matsuda, M. Arita, T. Uemura, M. Yamamoto, Y. Miura, M. Shirai, T. Saito, F. Shi, and P. M. Voyles, Phys. Rev. B **89**, 014428 (2014).
[26]J.-P. Wüstenberg, R. Fetzer, M. Aeschlimann, M. Cinchetti, J. Minár, J. Braun, H. Ebert, T. Ishikawa, T. Uemura, and M. Yamamoto, Phys. Rev. B **85**, 064407 (2012).
[27]V. R. Singh, V. K. Verma, K. Ishigami, G. Shibata, T. Kadono, A. Fujimori, D. Asakura, T. Koide, Y. Miura, M. Shirai, G.-f. Li, T. Taira, and M. Yamamoto, Phys. Rev. B **86**, 144412 (2012).
[28]Y. Ebina, T. Akiho, H-x. Liu, M. Yamamoto, and T. Uemura, Appl. Phys. Lett. **104**, 172405 (2014).
[29]Z. Lin, K. Kondo, M. Yamamoto, and T. Uemura, Jpn. J. Appl. Phys., Part 1 **55**, 04EN03 (2016).
[30]M. Rasly, Z. Lin, M. Yamamoto, and T. Uemura, AIP Adv. **6**, 056305 (2016).
[31]H. C. Torrey, Phys. Rev. **76**, 1059 (1949).
[32]R. A. Smith, Proc. R. Soc. London, Ser. A **362**, 1 (1978).
[33]A. Abragam, *The Principles of Nuclear Magnetism* (Clarendon Press, Oxford, 1961).
[34]H. Paik, S. K. Dutta, R. M. Lewis, T. A. Palomaki, B. K. Cooper, R. C. Ramos, H. Xu, A. J. Dragt, J. R. Anderson, C. J. Lobb, and F. C. Wellstood, Phys. Rev. B **77**, 214510 (2008).
[35]J. Fabian, A. Matos-Abiague, C. Ertler, P. Stano, and I. Žutić, Acta Phys. Slov. **57**, 565 (2007).
[36]D. Paget and V. L. Berkovits, in *Optical Orientation*, edited by F. Meier and B. P. Zakharchenya (North-Holland, New York, 1984).